ELSEVIER

Journal of Nuclear Materials 278 (2000) 225–232

journal of nuclear materials

www.elsevier.nl/locate/jnucmat

Near-field behavior of ^{99}Tc during the oxidative alteration of spent nuclear fuel

Fanrong Chen [a,c], Peter C. Burns [b], Rodney C. Ewing [a,*]

[a] *Department of Nuclear Engineering and Radiological Sciences, University of Michigan, Ann Arbor, MI 48109-2104, USA*
[b] *Department of Civil Engineering and Geological Sciences, University of Notre Dame, Notre Dame, IN 46556-0767, USA*
[c] *Guangzhou Insitute of Geochemistry, Chinese Academy of Sciences, Wushan, Guangzhou 510640, People's Republic of China*

Received 24 March 1999; accepted 24 September 1999

Abstract

^{99}Tc is a long-lived radioactive fission product with a half-life of 2.13×10^5 yr and a fission yield of 6.13% in nuclear reactors. ^{99}Tc is a prominent contributor to dose in safety assessments of nuclear waste repositories. Under Eh–pH conditions corresponding to the oxidative corrosion of spent nuclear fuel, which is constrained by the stability of uranyl phases relative to that of UO_{2+x} phases, TcO_4^- is the predominant species of technetium with $\log[TcO_4^-]/[TcO(OH)_2^0] > 2.15$ in the range of pH = 4–10. Because of the low solubility of $TcO_2 \cdot H_2O$ and high adsorption of Tc(4+) by geological materials and clays, the concentration of Tc(4+) in groundwater is expected to be less than 10^{-8} M, and the incorporation of Tc^{4+} into alteration uranyl phases is not considered to be an important retardation mechanism. In contrast, TcO_4^- is highly soluble and weakly adsorbed in the near-field. The incorporation of Tc^{7+} into the structure of uranyl phases that are expected to occur as alteration products of spent nuclear fuel will result in underbonding at the U^{6+} site and will destabilize the structure, suggesting that significant substitution of (TcO_4^-) will not occur in uranyl phases.

1. Introduction

Leaching experiments and natural analog studies have shown that the UO_2 in spent nuclear fuel is unstable under oxidizing environments and will alter to uranyl phases [1–6]. In the presence of an oxidizing aqueous phase, especially involving radiolytically produced oxidants, the alteration rate of spent fuel is likely to be appreciable [7–9]. The actinides and fission products associated with the altered fuel will be released from the UO_2 matrix, and the radioactivity and toxicity of long-lived actinides and fission products in spent fuel are then of environmental concern. Recent results of experiments on the oxidative dissolution of spent fuel indicate that some fission products, such as ^{137}Cs and ^{90}Sr, and actinides, such as Pu and Np, are incorporated into the uranyl alteration products [6,10]. Burns et al. [11] have proposed the probable incorporation mechanisms of actinides into U^{6+} phases. Our recent analysis has indicated that ^{79}Se released from altered spent nuclear fuel may also be incorporated into uranyl phases [12]. Due to these incorporation processes, the radioactive elements released during the oxidative dissolution of spent fuel may become immobilized in secondary U^{6+} phases.

^{99}Tc is a long-lived fission product with a half-life of 2.13×10^5 yr, and it is produced in appreciable amounts by fission of nuclear fuel [13]. The thermal neutron fission yield of 6.13% leads to a production of approximately 1 kg of ^{99}Tc for each ton of uranium fuel ($\approx$ 3% enriched) after burn-up. Although the longer half-life of ^{99}Tc results in a much lower radioactivity, as compared with ^{137}Ce and ^{90}Sr, ^{99}Tc still exhibits significantly greater radioactivity as compared with natural uranium ore. Therefore, the behavior and fate of ^{99}Tc released from the altered spent nuclear fuel is of great importance in the assessment of the performance of nuclear waste repositories.

* Corresponding author. Tel.: +1-734 647 8529; fax: +1-734 647 8531.
E-mail address: rodewing@umich.edu (R.C. Ewing).

0022-3115/00/$ - see front matter
PII: S0022-3115(99)00264-0

Mechanisms for the near-field immobilization of fission products include: (1) solubility-controlled precipitation of fission product-containing phases; (2) adsorption onto near-field geological and backfill materials; (3) incorporation as impurities into secondary phases formed during the corrosion of spent fuel. Because ^{99}Tc may exist in different oxidation states, redox (reduction–oxidation) reactions will cause changes in speciation of Tc that will have a marked effect on its mobility.

2. Eh–pH conditions for the oxidative corrosion of spent fuel

Natural analog studies suggest the long-term paragenesis of phases formed during the oxidative alteration of UO_2 fuel can be summarized as [3]: an initial decomposition of UO_2 to uranyl oxide hydrates followed by the formation of more stable uranyl silicates or, in phosphorous-rich groundwaters, the formation of uranyl phosphates. The sequence of phases formed by alteration as revealed in natural analog studies of uranium deposits can be used to propose the alteration conditions of spent fuel under a similar environment. For example, the geochemical environment of the Nopal I uranium deposit in the Peña Blanca district in Chihuahua, Mexico, is similar to that of the proposed HLW repository at Yucca Mountain [14]. Both the proposed Yucca Mountain repository and the Nopal I deposit are located in semi-arid to arid climate regions, composed of Tertiary rhyolitic tuffs underlain by carbonate sedimentary rocks and located in a hydrologically unsaturated zone 100 m or more above the water table. The mineral formation sequence in the Nopal I deposit is similar to that observed in other uranium deposits that have been summarized by Finch and Ewing [3]. Schoepite is the most common uranyl oxide hydrate in Nopal I and is followed or replaced by uranyl silicates, mainly uranophane and soddyite; becquerelite was identified by X-ray diffraction analysis but was not observed by optical microscopy. A similar suite of alteration phases has also been formed during the 10-yr drip test using Yucca Mountain EJ-13 groundwater on UO_2 [15].

The stability relations of the uranyl phases that occur in the Nopal I deposit in the SiO_2–CaO–UO_3–H_2O system are shown in Fig. 1, as well as the composition plots of J-13, EJ-13 and BH-12 groundwaters. Although the composition of the fluid involved in the alteration of the uraninite in the Nopal I deposit may be somewhat different from the BH-12, it does provide a reference for the regional geochemical background. Although precipitation of schoepite is kinetically favored in the early stage of alteration of uraninite in the Nopal I deposit, as has also been observed in other uranium deposits [3],

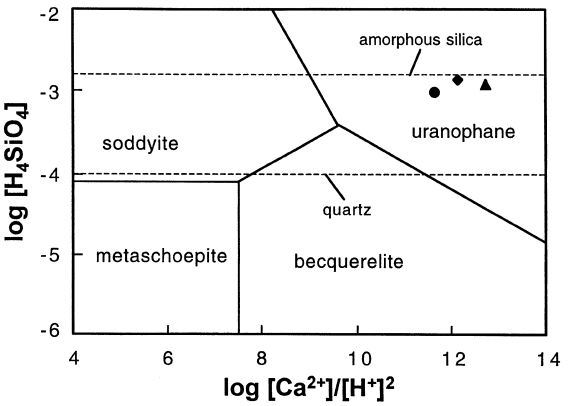

Fig. 1. Activity–activity diagram for SiO_2–CaO–UO_3–H_2O system showing the stability relations among uranyl phases frequently found in nature, with groundwater compositions of J-13 (●, from the J-13 well near Yucca Mountain [16]), EJ-13 (▲, J-13 groundwater equilibrated with tuff at 90°C for two weeks [4]) and BH-12 (◆, from a 10 m deep drillhole located about 20 m from the perimeter of the Nopal I deposit [14]). The thermodynamic data for the uranyl phases are from [17].

uranophane is the most stable alteration phase (Fig. 1). As the $\log[H_4SiO_4]$ and $\log[Ca^{2+}]/[H^+]^2$ decrease due to the precipitation of uranophane, soddyite will precipitate in this system. Occasional precipitation of becquerelite may occur due to the fluctuation of $\log[H_4SiO_4]$ and $\log[Ca^{2+}]/[H^+]^2$ in the solution resulting from soddyite and uranophane precipitation, fluid-host rock reaction, and variation in fluid flow. Thus, uranophane, soddyite and becquerelite are expected to be among the dominant minerals that will form during the oxidative alteration of spent nuclear fuel.

The surface composition of the UO_2 in spent fuel, which has the general formula UO_{2+x} $(0 < x < 1)$, depends on the redox potential at the fuel–water interface and has a significant influence on UO_2 dissolution [8]. X-ray measurements have shown that UO_{2+x} is an oxygen-excess structure with the extra oxygens occupying interstitial positions in the UO_2 lattice [19]. In the UO_2–U_4O_9 range, all the known phases have the fluorite structure, and as the composition deviates from UO_2, the unit-cell shrinks [20]. The more highly oxidized uranium, U_3O_7 (or $UO_{2.33}$), is tetragonal with a distorted fluorite structure that effectively marks the limit of the fluorite-structure range. Oxidation of the surface to $UO_{2.5}$ or $UO_{2.67}$ occurs by a recrystallization process involving a thin layer of $UO_{2.33}$ and adsorbed uranyl species [21]. Only under very aggressive oxidation conditions, almost certainly unachievable under disposal conditions, will UO_2 be oxidized to these higher oxide compositions. Thus, $UO_{2.5}$ and $UO_{2.67}$ are not expected to be present as intermediates during the alteration of

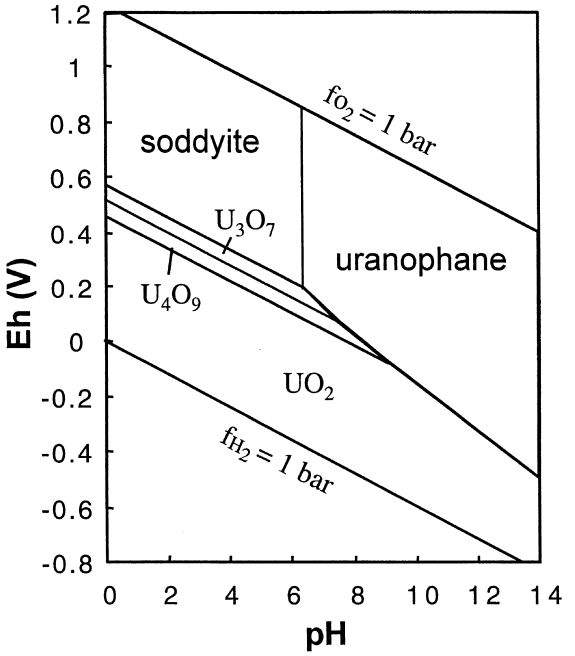

Fig. 2. Eh–pH diagram showing the stability relations among uranium phases equilibrated with Yucca mountain J-13 groundwater. The thermodynamic data for the uranyl phases are from [17]; those for the uranium oxides are from [18].

UO_2 under oxidizing conditions. Therefore, the stability fields of uranophane, soddyite and becquerelite relative to UO_{2+x} ($0 < x < 0.33$) in spent fuel are used as reference conditions to define the redox reactions of fission products and actinides in this study (Fig. 2). Because the Si concentration in J-13 groundwater is rather high (Fig. 1), becquerelite is a metastable phase and is not shown in Fig. 2.

3. Speciation of technetium

Technetium is anthropogenic. All isotopes of technetium are unstable and the amount of primordial Tc remaining in the Earth's crust is too small to be detected. There are several long-lived isotopes of technetium with half-lives over 10^5 yr. Among them, ^{99}Tc is of great environmental concern due to its high fission yield and potential mobility.

Technetium has a $4d^5 5s^2$ electronic configuration. The seven electrons occupying the outer orbits make possible valence states between 0 and +7. Species of oxidation state −1 have also been identified [22–24]. The most stable oxidation state of technetium is +7, and the next most stable is +4 [22,24]. In general, technetium species with oxidation states less than +4 are rapidly oxidized to Tc(4+) or ultimately to Tc(7+), while those with oxidation state between +4 and +7 usually disproportionate to a corresponding mixture of Tc(4+) and Tc(7+). Technetium's geochemical behavior and crystallo-chemical retardation by secondary phases depends largely on its oxidation state.

The predominance distribution of aqueous technetium species in an Eh–pH diagram is shown in Fig. 3. Equilibrium lines between uranyl phases and UO_{2+x} phases and the Eh–pH plots of some groundwaters reported by Lieser and Bauscher are also shown [25]. Under reducing conditions, the predominance ranges of hydrolyzed Tc(4+) species have been summarized as [22]: $pH < 1.5$, TcO^{2+}; $1.5 < pH < 2.2$, $Tc(OH)^+$ and $TcO(OH)_2^0$; $pH > 2.2$, $TcO(OH)_2^0$ and $[TcO(OH)_2^0]_2$; $pH > 3$, precipitation of $TcO_2 \cdot 2H_2O$. The predominance field for $TcO(OH)_2^0$ is close to the precipitation field of amorphous $Tc_2O \cdot H_2O$ at an activity of dissolved technetium of 10^{-8}. Fig. 3 shows that in the stability fields of uranyl phases, TcO_4^- is the dominant species, and the plots of the groundwater compositions fall in the TcO_4^- predominance field.

$TcO(OH)_2^0$ is the dominant species of Tc(4+) at $pH > 3$ and has the following relationship with TcO_4^-:

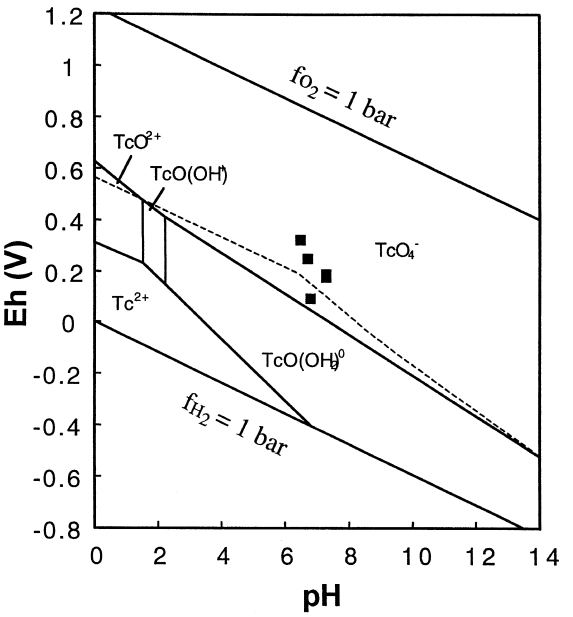

Fig. 3. Eh–pH predominance diagram for the aqueous species of technetium with the Eh–pH plots of some groundwaters reported by Lieser and Bauscher [25]. The thermodynamic data for technetium species are from [22]. The dashed lines represent the equilibrium between uranyl phases and UO_{2+x} as defined in Fig. 2.

$$TcO(OH)_2^0 + H_2O = TcO_4^- + 4H^+ + 3e^- \quad (1)$$

and

$$\log[TcO_4^-]/[TcO(OH)_2^0] = 50.6786Eh - 29.645 + 4pH, \quad (2)$$

where $[TcO_4^-]$ and $[TcO(OH)_2^0]$ are activities of the relevant species. If the Eh–pH conditions in the near-field are buffered by the reactions between uranyl phases and UO_{2+x} we have the following relations:

$$\begin{aligned}\log[TcO_4^-]/[TcO(OH)_2^0] &= pH - 0.74 && (3 < pH \leqslant 6.36)\\ &= -1.25pH + 13.57 && (6.36 < pH \leqslant 7.54)\\ &= -pH + 11.68 && (7.54 < pH \leqslant 9.09)\\ &= -0.5pH + 7.15 && (pH > 9.09).\end{aligned} \quad (3)$$

In the pH range of 4–10, the $\log[TcO_4^-]/[TcO(OH)_2^0]$ is greater than 2.15. This indicates that the activity of TcO_4^- is several orders of magnitude greater than that of $TcO(OH)_2^0$ over a wide range of pH.

4. Geochemical retention

Under reducing conditions, Tc(4+) is the dominant oxidation state. In the range of pH = 3–9, the predominant species in solution is either the hydrolysis species $TcO(OH)_{2(aq)}$ or the carbonate species $Tc(OH)_2CO_{3(aq)}$, and the solubility of $TcO_2 \cdot nH_2O$, i.e., the equilibrium concentrations of the predominant species, are very low and independent of pH (cf. [26,27]):

$$\log[TcO(OH)_{2(aq)}] = -8 \sim -9 \quad (\text{Refs. } [26,27]), \quad (4)$$

$$\log[Tc(OH)_2CO_{3(aq)}], = -7.1 + \log f_{co_2} \quad (\text{Ref. } [27]).$$

Because of the low solubility of $TcO_2 \cdot nH_2O$ and high sorption ratios of Tc(4+) aqueous species by geological materials [28–31] and by humic substances [32], Tc(4+) is immobile in most groundwaters and is not expected to be transported to the far field in significant amounts.

Under non-reducing condition, Tc(7+) is the stable oxidation state of technetium with TcO_4^- being the predominant species in aqueous solutions. The high solubilities ($\sim 10^{-1}$ mol) of Tc_2O_7 and the salts of TcO_4^- [24] make the solubility of Tc(7+) practically unlimited in near-field geochemical environments. However, the concentration of TcO_4^- may be limited by the solubility of $TcO(OH)_2^0$ via Eqs. (1) and (2). The upper limit for log $[TcO(OH)_2^0]$ may be $-8 \sim -9$ due to the low solubility of $TcO_2 \cdot nH_2O$ and sorption onto backfill clays and geological materials. Therefore, if the Eh–pH conditions in the near-field are buffered by the reactions between uranyl phases and UO_{2+x} (the actual conditions may be more oxidative), the concentration of log $[TcO_4^-]$ is estimated to be in the range of -3 to -6 at pH = 4–10.

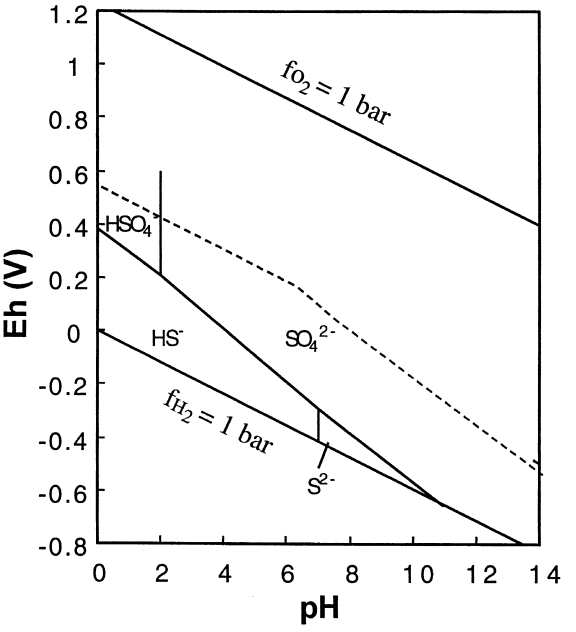

Fig. 4. Eh–pH predominance diagram for the aqueous species of sulfur with the equilibrium boundary between uranyl phases and UO_{2+x} given as a reference (dashed line).

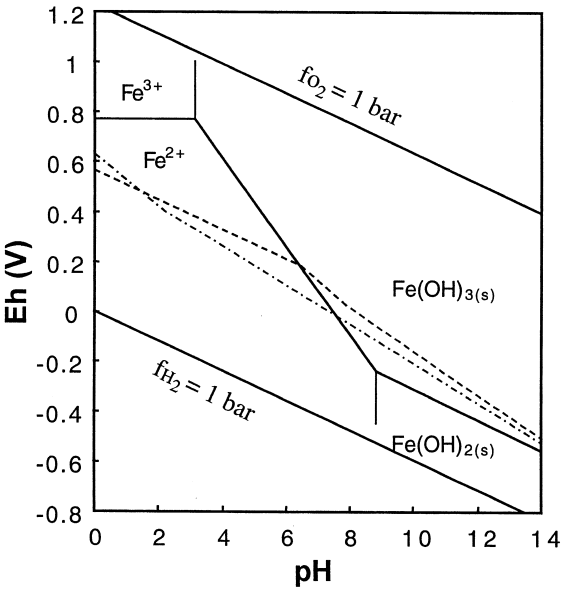

Fig. 5. Eh–pH diagram showing the distribution of chemical species of iron in aqueous solution. The 'dash–dot' line represents the boundary between $Tc(7+)_{(aq)}$ and $Tc(4+)_{(aq)}$ as shown in Fig. 3; the dashed line represents the equilibrium between uranyl phases and UO_2 as shown in Fig. 2.

Experimental studies indicated little sorption of TcO_4^- by geological and backfill materials [28,30,33,34] or by humic substances [32]. Thus, TcO_4^- is very mobile and will not be retarded by geological materials under the conditions of oxidative alteration of UO_2.

Some experiments suggested that the presence of sulfide may immobilize the dissolved TcO_4^- due to the formation of Tc_2S_7 [30,31] and that TcO_4^- may be reduced by ferrous iron to less mobile Tc(4+) in the near-field [31]. However, under the Eh–pH conditions typical of the oxidative alteration of spent UO_2 fuel, SO_4^- is the dominant species of sulfur (Fig. 4), and the concentration of S^{2-} is too low for Tc_2S_7 to precipitate. In neutral to alkaline solutions, ferrous iron may reduce TcO_4^- to Tc(4+). Shortly after the closure of a repository, oxidation of canister and engineered steel may cause the reduction of Tc(7+) to Tc(4+). However, this redox couple will not persist over the long-term because under the Eh conditions for the oxidative dissolution of spent fuel, ferrous iron is not stable and will be oxidized to ferric iron (Fig. 5).

5. Impact of uranyl alteration phases on the mobility of technetium

5.1. The crystal chemistry of U^{6+}

In order to evaluate the possibility of Tc incorporation into uranyl phases, a detailed understanding of the crystal-chemical behavior of U^{6+} is essential. The crystal chemistry of U^{6+} is complex owing in part to the variability of the coordination polyhedra around U^{6+}. The U^{6+} cation almost invariably occurs as part of an approximately linear $(U^{6+}O_2)^{2+}$ uranyl ion (designated Ur) [35], which is in turn coordinated by from four to six additional anions at the equatorial positions around the uranyl ion, resulting in square, pentagonal, and hexagonal bipyramids, designated Urϕ_4 Urϕ_5, and Urϕ_6, respectively [36].

Bond-valence considerations [36,37] indicate that the bonding requirements of the O_{Ur} atoms are largely met by the strong U^{6+}–O bond of the uranyl ion; thus the O_{Ur} anions may bond to interstitial low-valence cations or accept hydrogen bonds, but never bond to additional cations of higher bond-valence. However, the equatorial anions receive only ~ 0.5 valence units from the U^{6+} cations at the center of the polyhedra, and further bonding is required by these anions. As such, the equatorial anions are often bonded to another U^{6+} cation or other cation of high bond-valence, resulting in the polymerization of higher bond-valence polyhedra dominantly in two dimensions via the sharing of equatorial edges or corners [36,38]. Burns et al. [38] proposed a structural hierarchy for 180 phases containing U^{6+} as a necessary structural constituent. The hierarchy is based upon the polymerization of cation polyhedra of higher bond-valence. The most important class contains structures that are based upon infinite sheets of polyhedra, although structures containing isolated polyhedra, finite clusters of polyhedra, infinite chains of polyhedra, and frameworks of polyhedra also occur [38].

Table 1
Uranyl phases found as alteration products of UO_2

Structure known	
schoepite	$[(UO_2)_8O_2(OH)_{12}](H_2O)_{12}$
becquerelite	$Ca[(UO_2)_3O_2(OH)_3]_2(H_2O)_8$
compreignacite	$K_2[(UO_2)_3O_2(OH)_3]_2(H_2O)_8$
billietite	$Ba[(UO_2)_3O_2(OH)_3]_2(H_2O)_4$
soddyite	$(UO_2)_2(SiO_4)(H_2O)_2$
Na–boltwoodite	$(Na,K)(H_3O)[(UO_2)(SiO_4)]$
sklodowskite	$Mg[(UO_2)(SiO_3OH)]_2(H_2O)_6$
uranophane	$Ca[(UO_2)(SiO_3OH)]_2(H_2O)_5$
haiweeite	$Ca(UO_2)_2Si_6O_{15}(H_2O)_5$
Structure not known	
Dehydrated schoepite	$UO_3(H_2O)_{0.8–1.0}$

The phases listed in Table 1 are expected to form due to the alteration of spent nuclear fuel in a geological repository where oxidizing conditions exist, and each, with the exception of soddyite, has a structure that is based upon infinite sheets of high bond-valence polyhedra. In each of these structures, the interlayer regions contain low-valence cations and H_2O groups. Here we provide a brief review of the structures of these phases, as a knowledge of the structures is of paramount importance for the prediction of potential radionuclide-incorporation mechanisms.

5.1.1. Schoepite

All of the U^{6+} present in the structure of schoepite [39] is present as uranyl ions that are further coordinated by five anions, giving pentagonal bipyramidal arrangements. The uranyl polyhedra share equatorial edges and corners, resulting in the sheets illustrated in Fig. 6(a). The sheets, with composition $[(UO_2)_8O_2(OH)_{12}]$, are neutral and the interlayer of the structure contains only H_2O groups. The sheets of uranyl polyhedra are connected to each other by H bonding only.

5.1.2. Becquerelite and compreignacite

The structures of becquerelite [40] and compreignacite [41] contain topologically identical sheets of edge-sharing Urϕ_5 pentagonal bipyramids (Fig. 6(b)). The interlayers of the structures contain Ca and K or Na cations that are coordinated by O_{Ur} anions of the adjacent sheets of uranyl polyhedra and H_2O groups that are located in the interlayer.

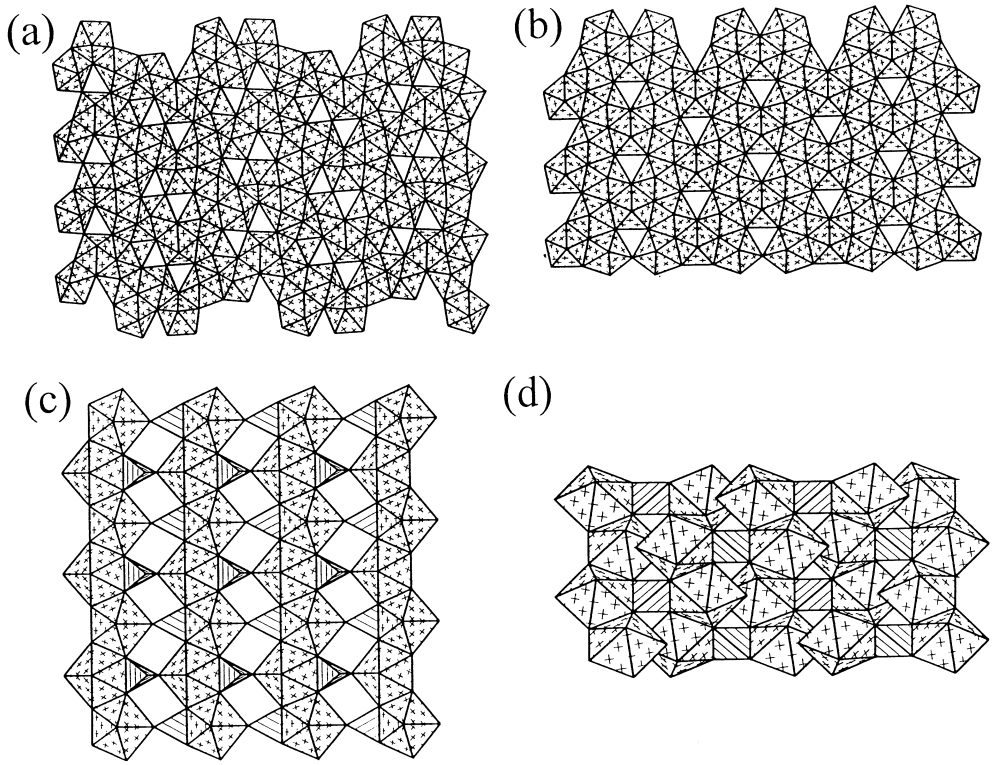

Fig. 6. Sheets occurring in the uranyl phases that were found as alteration products of UO_2: (a) schoepite; (b) becquerelite and compreignacite; (c) α-uranophane and boltwoodite; (d) soddyite.

5.1.3. α-Uranophane, boltwoodite, and sklodowskite

The structures of α-uranophane [42], boltwoodite [43], and sklodowskite [44] all contain the sheet of edge-sharing $Ur\phi_5$ pentagonal bipyramids and $Si\phi_4$ tetrahedra illustrated in Fig. 6(c). These structures contain Ca, Mg, K or Na in the interlayers, as well as H_2O groups. The anion topology of this mixed-polyhedral sheet is compatible with a wide variety of cation populations [38]; 10 unique sheets that occur in 16 different structures are based upon this anion topology.

5.1.4. Soddyite

The structure of soddyite [45] is unusual in that it consists of a framework of polyhedra, rather than being based upon sheets of polyhedra, which is usually the case for uranyl minerals [38]. The structure contains $Ur\phi_5$ pentagonal bipyramids that share edges to form chains, which are cross-linked by sharing edges with SiO_4 tetrahedra (Fig. 6(d)).

5.2. Incorporation of Tc

Hypothetically, the incorporation of Tc^{4+} and Tc^{7+} into the structures of uranyl phases must occur by incorporation into the sheets of polyhedra of higher bond-valence, as high-valence cations do not occur in the interlayers of any of the uranyl phases that are expected to form as a result of the alteration of UO_2 under oxidizing conditions.

In the phases listed in Table 1 that may form in quantities during the oxidative alteration of spent fuel, Tc^{4+} may substitute for the Si^{4+} in tetrahedral coordination. The effective ionic radius of $^{[4]}Tc^{4+}$ is unknown, but the effective ionic radius of $^{[6]}Tc^{4+}$ is 0.065 nm [46], which is 1.6 times larger than that of $^{[6]}Si^{4+}$. The significant difference in the effective ionic radii of Tc^{4+} and Si^{4+} implies that the substitution of Tc^{4+} for Si^{4+} is unlikely to occur. In addition, the concentration of Tc(4+) in solution is low due to the very low solubility of $TcO_2 \cdot nH_2O$ and efficient sorption of Tc(4+). Therefore, the incorporation of Tc^{4+} into uranyl phases is not considered to be an important retardation mechanism for technetium in the near-field.

Is it possible for the TcO_4 tetrahedron to exist within the sheets of uranyl polyhedra that occur in the structures of most uranyl phases? To do so, the tetrahedron must share an oxygen atom with at least one uranyl polyhedron within the sheet. Owing to the high charge on the Tc cation, a substantial amount of the bonding potential of the O atoms of the tetrahedron is satisfied

by the Tc^{7+}–O bond. Each Tc^{7+}–O bond has a formal bond-valence of 1.75 *vu* (i.e., 7/4), thus the O atoms of the tetrahedron can only provide ~ 0.25 *vu* for additional bonds.

The typical bond-valences associated with the equatorial U^{6+}–ϕ bonds of uranyl polyhedra can easily be calculated. To do this, we have used the bond-valence parameters and average polyhedral geometries provided by Burns et al. [36]. In order for a structure to be stable, the equatorial U^{6+}–ϕ bonds must provide about 0.69, 0.53, and 0.43 *vu* for $Ur\phi_4$ square bipyramids, $Ur\phi_5$ pentagonal bipyramids, and $Ur\phi_6$ hexagonal bipyramids, respectively. However, the O atoms of the TcO_4 tetrahedron can only contribute ~ 0.25 *vu* towards the requirements of the U^{6+} cation, thus a structure in which a TcO_4 tetrahedron is connected to a uranyl polyhedron will be unstable due to underbonding at the U^{6+} position.

All of the uranyl phases listed in Table 1 possess highly polymerized structures, hence we conclude that it is highly unlikely that significant Tc^{7+} can occur in any of these structures.

In the drip corrosion test of spent fuel under oxidizing conditions, retardation of actinides, Ce^{+} and Sr^{2+} by the secondary uranyl phases was observed [6]. However, the release rate of Tc was 2–3 orders magnitude higher than that of Ce and Sr and probably reflects the dissolution rate of the UO_2 matrix [6]. This provides experimental evidence to support the conclusion that Tc^{7+} release was not retarded by the formation of uranyl phases.

6. Conclusions

Under the Eh–pH conditions for the oxidative alteration of UO_{2+x}, TcO_4^- is the predominant species of technetium with $\log [TcO_4^-]/[TcO(OH)_2^0] > 2.15$ in the range of pH = 4–10.

Because of the low solubility of $TcO_2 \cdot H_2O$ and high adsorption of Tc(4+) by geological materials and clays, the concentration of Tc(4+) in groundwater is expected to be less than 10^{-8} M, and the incorporation of Tc^{4+} into alteration uranyl phases is not considered to be an important retardation mechanism.

TcO_4^- is highly soluble and weakly adsorbed in the near-field. The incorporation of Tc^{7+} into the structure of uranyl phases that are expected to occur as alteration products of UO_2 in spent nuclear fuel is only feasible by substitution for the high-valence cations, such as Si^{4+}. These cations are coordinated by four anions in the uranyl phases. The oxygens of the TcO_4 tetrahedron have much of their bond-valence requirement satisfied and can only contribute ~ 0.25 *vu* towards the requirements of U^{6+} to which the SiO_4 tetrahedra are linked. Thus, the substitution $TcO_4 \leftrightarrow SiO_4$ will result in underbonding at the U^{6+} position and will destabilize the structure, suggesting that significant substitution of (TcO_4^-) cannot occur in uranyl phases.

Acknowledgements

This research was funded by the Environmental Management Sciences Program of the United States Department of Energy [DE-FG07-97ER-14816 (RCE) and DE-FG07-97ER14820 (PCB)].

References

[1] C. Frondel, Systematic Mineralogy of Uranium and Thorium, US Geological Survey Bulletin 1064, US Government Printing Office, Washington, DC, 1958.
[2] R.J. Finch, R.C. Ewing, Radiochim. Acta 52&53 (1991) 395.
[3] R.J. Finch, R.C. Ewing, J. Nucl. Mater. 190 (1992) 133.
[4] D.J. Wronkiewicz, J.K. Bates, T.J. Gerding, E. Veleckis, J. Nucl. Mater. 190 (1992) 107.
[5] L.H. Johnson, L.O. Werme, MRS Bull. 19 (2) (1994) 24.
[6] P.A. Finn, J.C. Hoh, S.F. Wolf, S.A. Slater, J.K. Bares, Radiochim. Acta 74 (1996) 65.
[7] W.M. Murphy, E.C. Pearcy, in: C.G. Sombret (Ed.), Scientific Basis for Nuclear Waste Management XV, Proceedings of the Materials Research Society Symposium, vol. 257, 1992, p. 521.
[8] D.W. Shoesmith, S. Sunder, J. Nucl. Mater. 190 (1992) 20.
[9] S. Sunder, D.W. Shoesmith, M. Kolar, D.M. Leneveu, in: I.G. McKinley, C. McCombie (Eds.), Scientific Basis for Nuclear Waste Management XXI, Proceedings of the Materials Research Society Symposium, vol. 506, Materials Research Society, 1998, p. 373.
[10] E.C. Buck, R.J. Finch, P.A. Finn, J.K. Bates, in: I.G. McKinley, C. McCombie (Eds.), Scientific Basis for Nuclear Waste Management XXI, Proceedings of the Materials Research Society Symposium, vol. 506, Materials Research Society, 1998, p. 87.
[11] P.C. Burns, R.C. Ewing, M.L. Miller, J. Nucl. Mater. 245 (1998) 1.
[12] F. Chen, P.C. Burns, R.C. Ewing, J. Nucl. Mater. 275 (1999) 81.
[13] K.H. Lieser, Radiochim. Acta 63 (1993) 5.
[14] E.C. Pearcy, J.D. Prikryl, W.M. Murphy, Appl. Geochem. 9 (1994) 713.
[15] D.J. Wronkiewicz, J.K. Bates, S.F. Wolf, E.C. Buck, J. Nucl. Mater. 238 (1996) 78.
[16] C.J. Bruton, H.F. Shaw, in: M.J. Apted, R.E. Westerman (Eds.), Scientific Basis for Nuclear Waste Management XI, Proceedings of the Materials Research Society Symposium, vol. 112, Materials Research Society, 1988, p. 485.
[17] F. Chen, R.C. Ewing, S.B. Clark, Am. Mineral. 84 (1999) 650.
[18] I. Grenthe, J. Fuger, R.J.M. Konings, R.J. Lemire, A.B. Muller, C. Nguyen-Trung, H. Wanner, Chemical Thermo-

dynamics of Uranium, North-Holland, Amsterdam, 1992, p. 173.
[19] F. Gronvold, J. Inorg. Nucl. Chem. 1 (1955) 357.
[20] D.K. Smith, B.E. Scheetz, C.A.F. Anderson, K.L. Smith, Uranium 1 (1982) 79.
[21] S. Sunder, D.W. Shoesmith, M.G. Bailey, F.W. Stanchell, N.S. Mcintyre, J. Electroanal. Chem. 130 (1981) 163.
[22] J.A. Rard, Critical Review of chemistry and thermodynamics of technetium and some of its inorganic compounds and aqueous species, Report UCRL-53440, Lawrence Livermore National Laboratory, Livermore, CA, 1983.
[23] R. Colton, The Chemistry of Rhenium and Technetium, Wiley, New York, 1965, p. 12.
[24] K. Schwochau, Radiochim. Acta 32 (1983) 139.
[25] K.H. Lieser, C.H. Bauscher, Radiochim. Acta 42 (1987) 205.
[26] R.E. Meyer, W.D. Arnold, F.I. Case, G.D. O'Kelley, Radiochim. Acta 55 (1991) 11.
[27] T.E. Eriksen, P. Ndalamba, J. Bruno, M. Caceci, Radiochim. Acta 58&59 (1992) 67.
[28] B. Allard, H. Kipatsi, B. Torstenfelt, Radiochim. Radioanalyt. Lett. 37 (1979) 233.
[29] E.A. Bondietti, C.W. Francis, Science 203 (1979) 1337.
[30] K.H. Lieser, C.H. Bauscher, Radiochim. Acta 44&45 (1988) 125.
[31] S. Kunze, V. Neck, K. Gompper, Th. Fanghänel, Radiochim. Acta 74 (1996) 159.
[32] C. Wolfrum, K. Bunzl, J. Radioanalyt. Nucl. Chem. Articles 99 (1986) 315.
[33] T.T. Vandergraaf, K.V. Tichnor, I.M. George, in: G.S. Baeney et al. (Eds.), Geochemical Behavior of Disposed Radioactive Waste, American Chemical Society, Washington, DC, 1984, p. 25.
[34] J.W. Shade, L.L. Ames, J.E. MCGarrah, in: G.S. Baeney et al. (Eds.), Geochemical Behavior of Disposed Radioactive Waste, American Chemical Society, Washington, DC, 1984, p. 43.
[35] H.T. Evans Jr., Science 141 (1963) 154.
[36] P.C. Burns, R.C. Ewing, F.C. Hawthorne, Can. Mineral. 35 (1997) 1551.
[37] I.D. Brown, in: M. O'Keeffe, A. Navrotsky (Eds.), Structure and Bonding in Crystals, vol. II, Academic Press, New York, 1981, p. 1.
[38] P.C. Burns, M.L. Miller, R.C. Ewing, Can. Mineral. 34 (1996) 845.
[39] R.J. Finch, M.A. Cooper, F.C. Hawthorne, R.C. Ewing, Can. Mineral. 34 (1996) 1071.
[40] M.K. Pagoaga, D.E. Appleman, J.M. Stewart, Am. Mineral. 72 (1987) 1230.
[41] P.C. Burns, Can. Mineral. 36 (1998) 1061.
[42] D. Ginderow, Acta Crystallogr. C 44 (1988) 421.
[43] P.C. Burns, Can. Mineral. 36 (1998) 1069.
[44] R.R. Ryan, A. Rosenzweig, Cryst. Struct. Commun. 6 (1977) 611.
[45] F. Demartin, C.M. Gramaccioli, T. Pilati, Acta Crystallogr. C 48 (1992) 1.
[46] R.D. Shannon, Acta Crystallogr. A 32 (1976) 751.